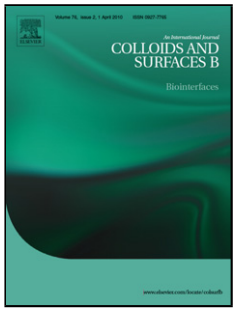

Title: Nanopolymersomes as potential carriers for rifampicin pulmonary delivery

Author: Marcela A. Moretton Maximiliano Cagel Ezequiel Bernabeu Lorena Gonzalez Diego A. Chiappetta

PII: S0927-7765(15)30279-4
DOI: http://dx.doi.org/doi:10.1016/j.colsurfb.2015.10.049
Reference: COLSUB 7451

To appear in: *Colloids and Surfaces B: Biointerfaces*

Received date: 16-9-2015
Revised date: 28-10-2015
Accepted date: 30-10-2015

Please cite this article as: Marcela A.Moretton, Maximiliano Cagel, Ezequiel Bernabeu, Lorena Gonzalez, Diego A.Chiappetta, Nanopolymersomes as potential carriers for rifampicin pulmonary delivery, Colloids and Surfaces B: Biointerfaces http://dx.doi.org/10.1016/j.colsurfb.2015.10.049

This revised version of the article entitled "Nanopolymersomes as potential carriers for rifampicin pulmonary delivery" by Marcela A. Moretton, Maximiliano Cagel, Ezequiel Bernabeu, Lorena Gonzalez and Diego A. Chiappetta. This article contains, including the abstract, 5,998 words, 3 tables and 4 figures.

Nanopolymersomes as potential carriers for rifampicin pulmonary delivery.

Marcela A. Moretton[1,3*], Maximiliano Cagel[1,3], Ezequiel Bernabeu[1,3], Lorena Gonzalez [2,3] and Diego A. Chiappetta[1,3]

[1] Department of Pharmaceutical Technology, Faculty of Pharmacy and Biochemistry, University of Buenos Aires, [2] Department of Biological Chemistry, Faculty of Pharmacy and Biochemistry, University of Buenos Aires, Argentina [3] Science Research Council (CONICET), Buenos Aires, Argentina

*Corresponding author
Dr. Marcela A. Moretton
Department of Pharmaceutical Technology, Faculty of Pharmacy and Biochemistry, University of Buenos Aires,
956 Junín St., 6th Floor,
Buenos Aires CP1113,
Argentina
Email: marcelamoretton@gmail.com
Phone/Fax: +54-11-4964-8371

Abstract

Tuberculosis (TB) has been stated as “the greatest killer worldwide due to a single infectious agent” behind the Human Immunodeficiency Virus. Standard short-term treatment includes the oral administration of a combination of “first-line” drugs. However, poor-patient compliance and adherence to the long-term treatments represent one of the mayor drawbacks of the TB therapy. An alternative to the oral route is the pulmonary delivery of anti-TB drugs for local or systemic administration. Nanotechnology offers an attractive platform to develop novel inhalable/respirable nanocarriers. The present investigation was focused on the encapsulation of rifampicin (RIF) (a “first-line” anti-TB drug) within nanopolymersomes (nanoPS) employing di- and tri-block poly(ethylene glycol) (PEG)-poly(ε-caprolactone) (PCL) based copolymers as biomaterials. The derivatives presented a number-average molecular weight between 12.2 KDa and 30.1 KDa and a hydrophobic/hydrophilic balance between 0.56-0.99. The nanoPS were able to enhance the apparent RIF aqueous solubility (up to 4.62 mg/mL) where the hydrodynamic diameters of the drug-loaded systems (1% w/v) were ranged between 65.8 nm and 94 nm at day 0 as determined by dynamic light scattering (DLS). Then, RIF-loaded systems demonstrated as excellent colloidal stability in aqueous media over 14 days with a spherical morphology as determined by transmission electron microscopy (TEM). Furthermore, RIF-loaded nano-sized PS promoted drug accumulation in macrophages (RAW 264.7) versus a drug solution representing promising results for a potential TB inhaled therapy.

Keywords: Nanopolymersomes; Rifampicin; Tuberculosis; Poly(ethylene glycol)-poly(epsilon-caprolactone) copolymer; Inhalable antitubercular therapy.

1. Introduction

Worldwide approximately 9 million people (64% newly diagnosed cases) became infected with *Mycobacterium tuberculosis* (*M. tuberculosis*) and 1.5 million died from the disease in 2013 **[1]**. Further, tuberculosis (TB) has been stated as "the greatest killer worldwide due to a single infectious agent" being the second most deadly infection only behind the Human Immunodeficiency Virus (HIV). Moreover, for HIV positive patients, TB has caused one fourth of HIV-related deaths **[1]**.

Actually, standard short-term treatment (6 months) comprises the oral administration of first line anti-TB drugs, rifampicin (RIF), isoniazid, pyrazinamide and ethambutol. This therapy consists of an initial (4 months) and continuous (2 months) phase to eradicate both, high- and low-replicant mycobacteria **[2-4]**. With a high patient adherence, treatment success is approximately 85%. However, daily administration of different anti-TB drugs for a long time leads to low patient compliance and treatment failure with *M. tuberculosis* resistance **[5]**.

A potential alternative to the oral route is the parenteral administration of anti-TB drugs. However, this is not a patient-friendly administration route due to the possibility of needle pain, infection risk and the requirement of trained staff **[6]**. Without treatment, TB mortality rates are high where HIV-negative patients usually die within 10 years (70%) **[7]**.

On the other hand, the inhalation of dry powders or nebulized suspensions that allow the drug delivery directly to the respiratory system for both, local and systemic drug administration represents an attractive alternative due to the possibility of increased anti-TB drugs concentration in the lungs (primary

infection site of *M. tuberculosis*). Also the reduction of side effects associated with oral administration of anti-TB drugs for long periods should be considered. Moreover, other benefits are related with the reduction of drug degradation along the gastrointestinal tract and an enhanced local bioavailability **[4, 8-10]**.

Nanotechnology represents a feasible platform where different approaches have been developed in order to evaluate inhalable nanocarriers based on biomaterials for pulmonary-related diseases as asthma, cystic fibrosis, lung cancer and even vaccines **[11-14]**. For TB treatment, the attention has been focused on nanoparticles, liposomes and micelles as drug delivery systems **[9]**.

Polymersomes (PS) are nano-sized vesicles made of the self-assembly of amphiphilic block copolymers. They consist in hollow spheres (aqueous core) surrounded by a bi-layer membrane where this membrane is composed of both i) hydrophilic polymer domains in contact with the external aqueous media and the internal aqueous core and ii) hydrophobic polymer domains between the hydrophilic ones **[15]**. In recent years, PS appear as versatile nano drug delivery systems since they can encapsulate hydrophilic (aqueous core), hydrophobic (bi-layer membrane) and amphiphilic drugs **[16,17]**.

Generally synthetic block copolymers-based PS have been investigated where differences in polymer average molecular weight and composition led to a variation in PS properties. Special focus has been made on PS due to their excellent colloidal stability which is mainly attributed to their macromolecular polymeric nature among others vesicular structures as liposomes, niosomes and polymeric micelles **[18]**. PS have demonstrated a greater mechanical stability and robustness than liposomes and they offer the possibility of surface modifications according to the employed synthetic polymer **[19-21]**. Then, these

characteristics highlighted potential applications of PS in medicine/biotechnology as versatile drug carriers especially in cancer chemotherapy **[22-25]**. Surprisingly, this nanotechnological platform has been not explored in the TB field.

In this framework, when combining nanopolymersomes PS (nanoPS) and their colloidal stability, they become excellent anti-TB drug carriers for pulmonary administration. Particular emphasis was place on the poorly-water soluble RIF encapsulation within PS since this is one of the most effective anti-TB drugs. RIF encapsulation within other nano-sized drug delivery systems has been already explored for oral, parenteral and inhalable administration **[9,26]**.

Herein, we proposed a novel, physically stable RIF-loaded nanoPS system employing biocompatible di- and tri-block copolymers of poly(ethylene glycol) (PEG)-poly(ε-caprolactone) (PCL) (PEG-PCL) as a nanotechnological platform for anti-TB pulmonary delivery. Derivatives were synthesized by ε-caprolactone ring opening polymerization (ROP) where nanoPS were obtained by a solvent-diffusion technique with and without sonication. The hydrodynamic diameter was assessed by dynamic light scattering (DLS) at 25 °C and RIF release profiles from PS were investigated using a membrane dialysis method. Further, *in vitro* quantitative analysis of the intracellular/cell RIF levels after its encapsulation within PS were assessed in murine macrophages. Finally, RIF encapsulation within PS for its potential pulmonary administration is reported for the first time to the best of our knowledge.

2. Materials and methods

2.1. Materials

ε-caprolactone (ε-CL), tin(II) 2-ethylhexanoate (SnOct) were purchased from Sigma-Aldrich (USA). Methoxy(polyethylene glycol) (mPEG, molar mass~5,000 g/mol) (mPEG 5000), poly(ethylene glycol) (molar mass~4,000 g/mol (PEG 4000); molar mass~6,000 g/mol (PEG 6000) and molar mass~10,000 g/mol (PEG10000)) was supplied by Merck Chemicals (Argentina). RIF was purchased from Parafarm® (Argentina). Solvents were of analytical or chromatographic grade and were used as received.

2.2. Copolymer synthesis

Block copolymers were synthesized by means of ring opening polymerization (ROP) of ε-CL initiated by mPEG 5000 or PEG (4000; 6000 and 10000) in the presence of SnOct (catalyst) **[27,28]**. Briefly, mPEG/PEG was poured into a round-bottom flask (250 mL) and dried under vacuum (100-120°C, 2 h) before use. Then, ε-CL (10% in molar excess) and SnOct (1:40 molar ratio to ε-CL) were added and mixed. The round-bottom flask was placed into a household microwave oven (Whirlpool®, WMD20SB, 800 W, Argentina, adapted in the laboratory to enable the connection of a condenser) and the reaction mixture was exposed to microwave irradiation **[27,28]** for 10 min under reflux. The crude was dissolved in dichloromethane (50 mL) and precipitated in hexane at room temperature (500 mL). The derivatives were isolated by filtration, washed several times with hexane, dried until constant weight at 25 °C and stored at 4 °C until use. The derivatives mPEG(5000)-PCL(7200), mPEG(5000)-PCL(12800), PCL(4000)-PEG(4000)-PCL(4000), PCL(6000)-PEG(6000)-PCL(6000) and PCL(10000)-PEG(10000)-PCL(10000) were denoted as di-

PCL(7200), di-PCL(12800), tri-PCL(4000), tri-PCL(6000) and tri-PCL(10000), respectively.

2.3. Copolymer characterization

The chemical composition of the derivatives was determined by means of proton nuclear magnetic resonance (^{1}HNMR). Briefly, ^{1}HNMR spectra were obtained from deuterated chloroform (Sigma) copolymer solutions on a Bruker MSL300 spectrometer (Germany), at 300 MHz. The chemical composition of each derivate was determined from ^{1}HNMR spectra where the hydrophobic/hydrophilic balance (CL/ethylene oxide (EO) molar ratio) and the number-average molecular weight (M_n) of the 5 derivatives were calculated by rationing the integration area of the peaks of PCL protons (2H, triplet, 2.30 ppm) and PEG (4H, multiplet, 3.65 ppm).

The thermal behavior of the different synthesized copolymers was analyzed by differential scanning calorimetry (DSC, Mettler Toledo TA-400, USA). Before the analysis, samples were heated at 100 °C (1 h) and cooled to 25 °C. Then, copolymers (4–7 mg) were sealed in 40 µL Al-cruicible pans and heated from 25 °C to 100 °C (10 °C/min). mPEG 5000 and PEG initiators (4000, 6000 and 10000) were analyzed for comparison. The melting temperature (T_m) and the normalized enthalpy of fusion (ΔH_m) were determined.

2.4. Preparation of RIF-loaded nanopolymersomes

NanoPS with RIF were prepared employing the different di- and tri-block copolymer synthesized by phase inversion (organic solvent-based method) with and without sonication **[18]**. Briefly, an organic solution of RIF (50 mg) and the copolymer (0.1 g) was obtained in acetone (7 mL). Afterwards the organic solution was added dropwise to distilled water (10 mL) under mechanical

stirring (three blade propeller, 1060 RPM) using a programmable syringe infusion pump (1mL/min, PC11UB, APEMA, Argentina) at room temperature. Mechanical stirring was continued for 1 h to ensure acetone evaporation **[27]** and the volume of the resulting aqueous dispersion was adjusted to 10 mL with distilled water in a volumetric flask. Then samples were sonicated (Digital Ultrasonic Cleaner, PS-10A 50/60 Hz, China, 15 min, 25 °C) and filtered (0.45 µm cellulose nitrate membranes). To prepare drug-free nanoPS, a similar procedure was followed, though without RIF addition to the acetone solution.

In order to compare between different preparation techniques, a similar method was followed to prepare RIF-free and drug-loaded nanoPS without the sonication step. In this case, after acetone evaporation samples were adjusted to 10 mL and filtered as described above.

The RIF concentration was determined by UV/Vis spectrophotometry (482 nm, CARY [1E] UV–Visible Spectropho-tometer, USA) using a calibration curve of RIF solutions in *N,N*-dimethylformamide (DMF) (3.125-50 µg/mL, R^2: 0.9998-0.9999). A drug-free copolymer solution in DMF was used as blank. Solubility factors (f_s) were calculated according to **Eq. (1)**

$$f_s = S_a / S_{water} \qquad \textbf{(1)}$$

Where, S_a and S_{water} are the apparent solubility of RIF in the corresponding PS dispersion and the drug experimental intrinsic solubility in distilled water at 25 °C (pH 5.0). Assays were carried out in triplicate and the results are expressed as mean ± S.D.

2.5. Size and size distribution analysis

The size and size distribution (polydispersity index, PDI) of drug-free and drug-loaded nanoPS (1% w/v copolymer) were measured by Dynamic Light

Scattering (DLS, Zetasizer Nano-Zs, Malvern Instruments, UK) provided with a 4mW He-Ne (633 nm) laser and a digital correlator ZEN3600, at 25 °C. Measurements were conducted at a scattering angle θ = 173° to the incident beam. Samples were equilibrated for 5 min at 25 °C prior to the analysis. Data was analyzed using CONTIN algorithms (Malvern Instruments) and the results of hydrodynamic diameter (D_h) and PDI are expressed as the average of three measurements.

2.6. Physical stability of the RIF-loaded nanopolymersomes

In order to evaluate the physical stability of the drug-free and RIF-loaded nanocarriers in aqueous media, samples (1 mL) were placed into sealed glass vials (5 mL) and stored at 25 °C for 14 days. At different timepoints (3, 7 and 14 days), the D_h and PDI values were evaluated by DLS as previously described.

2.7. Visualization of RIF-loaded nanopolymersomes using transmission electron microscopy.

The morphology of the RIF-loaded tri-PCL(4000) nanoPS (1% w/v) was characterized by means of transmission electron microscopy (Philips CM-12 TEM apparatus, FEI Company, The Netherlands). Samples (5 µL) were placed onto a grid covered with Fomvar film. After 30 sec, the excess was removed with filter paper and phosphotungstic acid (2% w/v, 5 µL) was added. Then, after 30 sec, the excess was removed and water (5 µL) was added for another 30 sec and removed. Finally samples were dried in a silica gel container and analyzed.

2.8. *In vitro* RIF release

The *in vitro* release profiles of RIF encapsulated within di-PCL(7200) and tri-PCL(4000) nanoPS were evaluated using a dialysis method. Briefly, the

aqueous dispersions of RIF-loaded (4 mg/mL) nanoPS (8 mL) were placed into dialysis membranes (Spectra/Por® Dialysis Membrane, molecular weight cut off = 3,500, nominal flat width 18 mm, USA) and immersed into the release medium (phosphate buffer USP 30 pH 7.4 with Tween 80 0.5 % v/v, 250 mL) for 6 h at 37 ± 1 °C under gentle magnetic stirring (100 RPM). At different time points (1, 2, 3, 4, 5 and 6 h) aliquots (50 µL) were removed from inside the dialysis membrane and RIF concentration was determined by UV/Vis spectrophotometry (CARY [1E] UV–Visible Spectropho-tometer, Varian, Palo Alto, California) at 482 nm. Then, the linearity range was established between 3.125 and 50 µg/mL (R^2: 0.9998-0.9999) where RIF solutions were prepared in DMF. Assays were carried out in triplicate and the results are expressed as mean ± S.D.

2.9. *In vitro* cellular uptake

A murine macrophage suspension (RAW 264.7, ATCC, USA, 2 mL) was added to each well of a 6-well plate to yield 200,000 cells/well. Afterwards, each plate was incubated (37 °C, 5% CO_2) for 24 h to allow cell attachment. Next, cells were washed with PBS (1 x 1mL, pH 7.4). Drug-loaded (4 mg/mL) tri-PCL(4000) nanoPS (1% w/v) were diluted with distilled water to a RIF concentration of 1 mg/mL and then aliquots (75 µL) were placed into each well and incubated for 0.5, 2, 4 and 6 h (37 °C, 5% CO_2). A RIF aqueous solution (1.9 mg/mL) was used as control.

For every time point, macrophages were washed with cold PBS (1.5 mL) in order to finish the uptake and the RIF-loaded dispersion was removed from each well. After cells were washed twice with PBS pH 7.4 (1 mL) and 0.25 mL trypsin PBS solution (2.5 µg/mL) was added. Cell lysates were collected and

centrifuged (13,000 RPM, 10 min, MiniSpin® plus™, Eppendorf, Germany). The supernatant was collected and 25 µL were used to assay soluble protein content (BCA protein assay kit, Pierce Corporation, China). Afterwards, 200 µL of the remaining supernatant were mixed with acetonitrile (200 µL) to precipitate proteins and samples were re-centrifuged (13,000 RPM, 10 min, MiniSpin® plus™, Eppendorf, Germany). Finally, supernatant was collected and the RIF concentration was determined by reverse-phase high performance liquid chromatography (RP-HPLC) as described below (2.10.). Statistical analysis was performed using one-way ANOVA test ($p<0.05$). Assays were carried out in triplicate and the results are expressed as mean ± S.D.

2.10. RP-HPLC analysis

The RIF intracellular/cell concentrations were determined by RP-HPLC employing an adapted analytical method **[29]**. Briefly, the method consisted of a reversed phase C18 column (4.6 mm x 250 mm, 5 µm, Fluophase PFP, Thermo, USA) with a C18 guard column and mobile phase of acetonitrile:TFA 0.1% (60:40, v/v). The flow rate was 1 mL/min and the injection volume was 100 µL. The linearity range was established between 0.05 µg/mL and 5 µg/mL (R^2: 0.997) with standard RIF solutions in acetonitrile:water (60:40, v/v). Finally the UV detection was performed at 333 nm (UV-detector, Shimadzu SPD-10A, Japan).

3. Results and discussion

3.1. Copolymer synthesis and characterization.

One of the main objectives of the present investigation was the development of amphiphilic block copolymers which could self-assemble into nanoPS in an aqueous media in order to encapsulate the poorly-water soluble RIF. It is well

known that amphiphilic copolymers can self-assemble in water into polymeric i) micelles or ii) PS, adopting different morphologies **[30]**. Since the PS obtention strongly depends on the relative lengths of the hydrophobic and hydrophilic copolymer domains, the average molecular weight, as well as on the method of PS preparation **[31]**, we synthesized derivatives with hydrophilic block/total copolymer mass (f_{PEG}) ratio of 35 ± 10 % in order to obtain PS instead of polymeric micelles (**Table 1**), as previously described for PEG-PLA di-block copolymers and PEG-PCL di- and tri-block copolymers **[30,32-34]**. Afterwards, we could successfully synthesize 5 amphiphilic derivatives (mPEG-PCL; PCL-PEG-PCL) (**Fig. 1**) where the main molecular properties of the different derivatives are summarized in **Table 1**. Additionally, the polymerization was assisted by microwave radiation as previously described **[27]**. Experimental results were in good concordance with the theoretical composition demonstrating high monomer conversion.

Since the thickness of the hydrophobic PS membrane can vary according to the polymer i) average molecular weight and ii) hydrophilic/hydrophobic balance **[35]**, we synthesized different PEG-PCL copolymers which exhibited M_n values between 12.2 and 30.1 KDa and CL/EO molar ratios in the range of 0.56-099 to evaluate their aqueous aggregation and RIF encapsulation (**Table 1**).

With the objective of gaining further insight of the thermal behavior of the different synthesized block copolymers which could influence their aggregation water-behavior, a DSC analysis was performed for every derivate and their corresponding PEG precursors for comparison (**Table 1**). Results showed a single endothermic peak for every sample assayed, denoting the absence of secondary crystal populations. Furthermore, data clearly denote a decrease on

both, T_m and ΔH_m values, after ε-CL polymerization with PEG. For example, the precursor mPEG 5000 exhibited T_m and ΔH_m values of 62 °C and 185.2 J/g, respectively; however, after PCL incorporation these values gradually decrease to 58 °C and 103.3 J/g for di-PCL(7200) and 59 °C and 86.9 J/g for di-PCL(12800). Notice that the decrease on ΔH_m values was more pronounced for the derivate with longer PCL segment demonstrating a higher detrimental effect on PEG crystallinity. A similar behavior was observed for the tri-block copolymers where all the derivatives presented the same CL/EO molar ratio (**Table 1**). For the three derivatives, the T_m values for the copolymers were lower than those observed for their PEG precursors. Further, the greater the total hydrophobic block, the more pronounced decrement on ΔH_m values, being this effect less marked for tri-PCL(10000) (**Table 1**). Overall, DSC data demonstrated that PEG crystallinity was decreased after its copolymerization with ε-CL.

3.2. Characterization of the nanoPS.

3.2.1. NanoPs preparation and physical stability of the aggregates.

PS have emerged as a novel nanotechnological strategy with high potential as drug delivery carriers in different investigations fields. Since TB has been positioned as the second most deadly infection behind the HIV infection **[1]**, it is surprising the fact that these versatile nano-sized carriers have not been already investigated for anti-TB drug encapsulation.

Different techniques have been developed to obtain PS for instance polymer re-hydration and solvent-diffusion/phase inversion technique **[18]**. In the present investigation we assay the solvent diffusion technique with and without the use of sonication. It has been established that PS size can be controlled by i) the

preparation method and ii) the employed polymer, where monomodal PS dispersions can be obtained with a phase inversion technique **[36,37]**. Moreover we combined the former method with sonication as an attempt to disrupt any large aggregates that could be obtained after the organic solvent evaporation **[38]**.

Firstly, we prepared drug-free nanoPS employing only an acetone-diffusion technique where the size and size distribution of the aggregates (copolymer 1% w/v) was determined by DLS over 14 days in aqueous media. Results demonstrated an unimodal size distribution for every copolymer assayed with PDI values ranged between 0.134 and 0.338 (day 0). For di-block based PS, an increase in the molecular weight mirrored a slight increase on vesicle size from 66.3 nm (di-PCL(7200)) to 72.8 nm (di-PCL(12800)) at day 0, respectively (**Table 2**). These results could be associated with the synthetic polymer employed since the M_n value could influence the PS size **[39]**. Here, both copolymers presented the same weight of hydrophilic block (mPEG 5000), however, di-PCL(12800) exhibited not only a greater M_n value but also a higher CL/EO molar ratio than di-PCL(7200), where the higher hydrophobic copolymer content, the greater membrane thickness of the PS **[17]**. Thereafter a higher D_h is expected for PS obtained with di-PCL(12800). Conversely, tri-block based PS did not follow the same behavior. In this case, there was not a clear difference on D_h between the derivatives at day 0. Only tri-PCL(4000) showed a higher D_h (92.8 nm; PDI: 0.338) in comparison with tri-PCL(6000) (75.6 nm; PDI: 0.250) and tri-PCL(10000) (75.7 nm; PDI: 0.174) (**Table 2**). However, tri-PCL(4000) demonstrated the highest PDI value of the series indicating that the colloidal system was not stable, thereby, an initial D_h higher than the other tri-block

copolymers was expected. This effect could be related with the weight of the hydrophilic block. Tri-PCL(4000) presented the shortest hydrophilic block of the serie, thereafter a size broad distribution was expected due to a weak corona repulsion. Similar behavior was observed by Ma and Eisenberg **[40]**. The absence of a difference on D_h values between tri-PCL(6000) and tri-PCL(10000) is probably related with the CL/EO ratio of the synthesized copolymer. Probably, the weight of the hydrophilic block (PEG 6000 and PEG 10000) is long enough to obtain a narrow size distribution. Moreover, the copolymer with PEG 10000, demonstrated a lower system polydispersity than its counterpart with PEG 6000 (**Table 2**). Further, both copolymers exhibited different M_n values but they presented the same CL/EO ratio (0.77), which could influence on the PS final size where only a difference of a few nanometers was observed (**Table 2**).

In order to asses the physical stability of the aggregates in aqueous media, the PS size and PDI values were determined over 14 days. Di-block based PS demonstrated an excellent colloidal stability where there was only a slight increase of both i) D_h and ii) PDI values as shown on **Table 2**. In contrast, tri-block based PS did not demonstrate the same physical stability as their di-block counterparts over time. Systems displayed a clear size growth for both, tri-PCL(4000) and tri-PCL(6000) block copolymers. This behavior for drug-free PS dispersions could be associated to vesicle aggregation over time, leading to a more physically unstable colloidal system which can be correlated with the appearance of generation of sub-micron particles as a second size population. For example, drug-free PS of tri-PCL(6000) showed a bimodal size distribution at day 7 (79.9 and 1839.0 nm) with an increment on PDI values from 0.250 to

1.000 over 14 days (**Table 2**). For tri-PCL(10000) a similar behavior was observed but drug-free PS dispersions did not exhibit a high tendency to undergo phase separation due to PS size enlargement. What is more, tri-PCL(10000) based PS demonstrated a higher colloidal stability than its tri-block counterparts, in a similar manner to di-block copolymers.

Among the tri-block derivatives, tri-PCL(10000) presented the highest M_n value (30.1 KDa) and the same f_{PEG} value (33.3 %). However, this copolymer contains PEG 10000 as hydrophilic block which could act as a steric barrier stabilizing the RIF-free polymeric vesicle into a greater extend than its counterparts PEG 6000 and PEG 4000, minimizing vesicle fusion **[17]**.

In a second stage, we introduced a sonication step in the nanoPS preparation technique as an attempt to obtain a monodisperse drug-free PS with a decrement on vesicle size. Conversely, results demonstrated that there was a slight augment on PS size at day 0 for di-block copolymers in comparison with those systems prepared in absence of sonication (**Table 2**). Then, for tri-block copolymers there was a bimodal size distribution with a dramatic size increment at day 0 in comparison with those colloidal dispersions prepared without sonication. These results correlated with the increment on PDI values for every tri-block copolymer assayed. For example, for tri-PCL(10000) the PS size enlarged from 75.7 nm to 73 nm and 373 nm before and after sonication at day 0, respectively. Also, the PDI values were increased from 0.174 to 0.465 without and with sonication, respectively (**Table 2**). Similar results were observed for PS prepared with a di-block copolymer of PEG and polybutadiene **[41]**.

Following a similar trend, colloidal systems did not show a better physical stability than their counterparts without sonication, especially for tri-block based

copolymers. It was observed an increment on system polydispersity and size growth over time (**Table 2**). The generation of sub-micron aggregates was favored in aqueous media where larger particles demonstrated a high tendency to undergo phase separation. These results could be associated with the implementation of the sonication step. PS size after their formation can be fine-tuned employing different methods as freeze-thaw cycles or sonication in order to disrupt any aggregates that could be obtained during the inversion phase technique **[38]**. Nevertheless, sonication is also known as a destabilizing method which may affect vesicle membrane-bound structures associated with cavitation **[41]**. Then the physical stability of the present nano sized PS assayed was decreased after the sonication cycle, leading to an increment on both, vesicle size and the polydispersity of the colloidal system. Furthermore a more polydisperse dispersion results more prone to undergo into secondary aggregation, vesicle fusion and precipitation in aqueous media over time.

Overall, results showed that a PS preparation technique involving a phase inversion technique without a sonication step would be the most appropriated method to obtain a more stable colloidal dispersion. Moreover this technique was employed to produce the RIF-loaded nanoPS.

3.2.2. Drug encapsulation.

In recent years, pulmonary anti-TB drug delivery has been in the spotlight due to the opportunity of developing a more effective anti-TB therapy. Additionally, an inhalable therapy could get a further insight into the *M. tuberculosis* non-replicant reservoirs in alveolar macrophages, optimizing the actual oral/parenteral therapy **[42]**.

Particularly, RIF exhibits two main (bio)pharmaceutical limitations such as its low pH-dependant aqueous solubility and its chemical instability under acid or basic conditions. The former limits the development of novel liquid RIF formulations. Further, drug degradation in acid conditions may decrease the drug bioavailability after an oral administration. Additionally, it has been established that the presence of isoniazid in the acid media catalyzed the RIF acid degradation, being this fact clinically relevant especially in the Fixed Dose Combination capsules **[43]**. Hence, RIF pulmonary administration within a nanocarrier could enhance its (bio)pharmaceutical limitations not only by improving drug aqueous solubility but also by avoiding the pH variation of the gastrointestinal tract. Besides RIF encapsulation within an inhalable nanocarrier would also promote its uptake by alveolar macrophages which constitute *M. tuberculosis* reservoirs **[44]**.

Aiming to explore the potential of inhalable PS to encapsulate the anti-TB drug RIF, the present investigation assessed the RIF solubility within PEG-PCL-based nanoPS.

First, we determined the drug S_{water} value employing the same technique used for the nanoPS preparation but without the addition of copolymers. Results demonstrated that the drug S_{water} value was 1.9 ± 0.03 mg/mL at pH 5.0. Then, the RIF solubility performance by the different nanoPS (copolymer concentration 1% w/v) dispersions was assessed. Data demonstrated that RIF could be encapsulated within nanoPS where drug solubility was increased up to 4.62 mg/mL (f_s: 2.71) at pH 5.0. When considering the di- and tri-block copolymers employed, there was only a slight variation on the f_s values between the different derivatives. For di-block copolymers, the S_a values ranged between

4.07 ± 0.05 mg/mL (f_s: 2.17) and 4.41± 0.04 mg/mL (f_s: 2.57) for di-PCL(7200) and di-PCL(12800), respectively. In a similar manner, tri-block derivatives showed f_s values of 2.71 (S_a 4.62 ± 0.02 mg/mL), 2.51 (S_a 4.41 ± 0.03 mg/mL) and 2.47 (S_a 4.37 ± 0.07 mg/mL) for tri-PCL(4000), tri-PCL(6000) and tri-PCL(10000), respectively. These results could be associated with the bulk RIF molecule (822.95 Da) **[45]** where the difference of M_n and CL/EO balance of the copolymers did not improve the RIF encapsulation into a greater extend.

If we compare the i) inhalable and ii) systemic administration of a drug, the first usually requires lower doses since inhaled drugs are localized in the target organ **[46]**. For TB, it has been demonstrated that the mean inhalable RIF concentration inside alveolar macrophages was higher (~113-fold) than the concentration achieved after a RIF oral administration in healthy adult volunteers **[47]**. Hence the daily oral maximum RIF dose of 600 mg (10 mg/kg body weigh) **[5]** could be considered as approximately 6 mg/day for the inhaled drug. Taking into account the RIF concentration in the developed nanoPS dispersion (4.62 mg/mL), the daily RIF concentration would be contained in only a PS dispersion volume of ~ 1.3 mL. Thereafter, this volume could be a feasible administration dose by nebulization in both, adults and children **[48]**. In this way, the RIF S_a values obtained could be sufficient to achieve a therapeutic effect. Interestingly, for a PS dispersion volume of 1.3 mL, only 13 mg of copolymer would be daily administered to a patient. This issue also exhibits clinical relevance as the effect of different pharmaceutical additives after their lung deposition in the middle-long term has not been well established yet **[42]**. Thus, it is critical to reduce the amount of copolymer daily administered in a potential respirable formulation. It is also worth stressing that PEG and PCL

biomaterials have been also investigated for the development of different nano/micro-sized pulmonary drug delivery systems **[49,50]**.

3.2.3 Size distribution, physical stability and morphology

In order to gain further insight on the size distribution of the RIF-loaded PS dispersions, we assessed the D_h values for every nanoPS formulation at day 0 (**Table 3**). Di-block based PS demonstrated nano-scale D_h values with a monomodal size distribution. If we compare the size between nanoPS before and after RIF encapsulation, there was a slight increase on D_h values for drug-loaded PS. Also RIF-loaded vesicle dispersions demonstrated a narrow size distribution with PDI values of 0.138 and 0.150 for di-PCL(7200) and di-PCL(12800), respectively (**Table 3**). Similar results were observed for tri-block based nanoPS. In this case, it was observed an unimodal size distribution with D_h values between 65.8 nm and 94.0 nm (**Table 3**). Remarkably, data showed a narrow size distribution where PDI values were ≤ 0.168, being these results different from those obtained for drug-free systems (0.174-0.338) (**Table 2**). The decrement on the polydispersity of the nanoPS dispersion could explain the decrease on D_h values for the RIF-loaded systems in comparison with their counterparts without drug, especially for tri-PCL(4000) and tri-PCL(6000) (**Table 2**). For tri-PCL(10000), although RIF-loaded systems exhibited lower PDI values than drug-free dispersions, there was a slight increase on D_h values after RIF encapsulation from 75.7 nm to 94.0 nm at day 0. Similar results were observed for PS with calcein **[51]**.

Since particle size constitutes a critical factor for cellular uptake where phagocytosis represents the main mechanism for active nanoparticle uptake by macrophages, our results could represent a feasible platform for pulmonary RIF

delivery. Moreover, recent studies have demonstrated that nanoparticles of ~50 nm could be easily uptaken than larger ones (>200 nm) **[52]**.

Further, we investigated the physical stability of the aggregates in the aqueous media. Since PS based of block-copolymers exhibited long shelf life **[53]**, we assessed the physical stability of RIF-loaded nanoPS over time. For every copolymer assayed, systems showed excellent colloidal stability where the D_h and PDI values remain almost unchanged over 14 days. There was a narrow size distribution over time without the appearance of secondary size populations (**Table 3**). Data strongly suggests that the RIF encapsulation within PS did not modify the colloidal stability of the aggregates over time.

To gain further insight on nanoPS morphology, a TEM microscopy assay was performed. It has been proposed that not only the size but also the shape of nano sized carriers could present a great influence on their cellular uptake **[54]**. In our study, drug-loaded nanoPS showed a spherical morphology, where it could be distinguished two different domains, probably corresponding to the hydrophobic and hydrophilic PS domains (**Fig. 2**). Due to the cellular uptake kinetics, spherical PS could be easier endocyted than rod-shaped ones, being their morphology another benefit to facilitate the RIF-loaded nanoPS uptake by macrophages. In addition, nanoPS presented a size of ~60 nm, being in good concordance with DLS data (**Table 3**).

3.3. *In vitro* RIF release

In order to characterize the *in vitro* RIF release from the nanoPS, we assessed the drug (4 mg/mL) release profiles from nanoPS systems over 6 h at 37 °C. Since it was not observed a clear difference on drug encapsulation between the 5 synthesized copolymers, we analyzed one di-block (di-PCL(7200)) and one

tri-block copolymer (tri-PCL(4000)) in order to compare if there was any difference on RIF release between copolymers with different block structure. Both derivatives were chosen, due to that i) RIF-loaded PS exhibited the smallest size among their series and ii) the PS dispersions presented a narrow size distribution (low PDI values) (**Table 3**). The RIF cumulative release profiles are represented on **Fig. 3**. All nanoPS formulations disclosed a sustained RIF release, while no burst effect was observed. In fact the amount of drug release over 3 h was ~19% and ~31% for di-PCL(7200) and tri-PCL(4000), respectively. Then after 6 h, the RIF cumulative release was ~43% and ~51%. It has been proposed that the molecular weight of copolymers represents a key factor on drug release rate from PS **[55]**. Data revealed that both copolymers presented a similar RIF release profile probably related to the fact that both derivatives showed the same M_n value and similar f_{PEG} values (**Table 1**). In this case, drug release from the nanoPS could be associated with the PS bilayer morphology where the water penetrates the hydrophobic PCL domain. Further PEG-PCL chains could control the vesicle disintegration and the drug release though vesicle swelling and passive poration **[32,37]**.

In terms of pulmonary drug delivery, promising results could be expected from this novel nanoPS system. The inhalable particle ability to release an anti-TB drug inside the alveolar phagocyte cells remains of clinical relevance since *M. tuberculosis* exhibits the ability to survive inside alveolar macrophages **[42]**. Thereafter, an immediately drug release from the colloidal system could promote drug systemic absorption through the lung epithelium **[10]**. However, *in vitro* RIF release data from the nanoPS systems demonstrated that the drug was not immediately released from the polymeric matrixes (RIF cumulative

release ≤ 31% after 3 h) (**Fig. 3**). Then, our system could be taken up by a phagocyte cell and RIF could be released inside the alveolar macrophage as an attempt to improve TB treatment.

3.4. *In vitro* macrophage uptake

Taking into account TB pathogenesis, one of the main clinical issues is the ability of *M. tuberculosis* to survive and replicate inside the host alveolar macrophages (mycobacteria reservoir). Conventional oral TB treatment could lead to i) poor pulmonary drug distribution and ii) low drug penetration into the granulomas **[9,56]**. One of the main goals of pulmonary drug administration is the passive intracellular delivery of anti-TB drugs to phagocytic cells to eradicate mycobacteria reservoirs. Moreover, bactericidal macrophage activation upon phagocytosis could be expected **[57]**. For this reason, we aimed to investigate whether our nanoPS system could be taken up by phagocytic cells. Then, the intracellular/cell RIF levels were assessed in RAW 264.7 employing a RIF final concentration of 50 µg/mL. First, a RIF control solution was assayed where the RIF intracellular/cell levels remain almost unchanged over 6 h (**Fig. 4**.). In this case, the drug intracellular/cell level was 1.43 µg/mg after 6 h. Then, based on the *in vitro* drug release data where both copolymers showed a similar RIF release profile, a drug-loaded tri-PCL(4000) nanoPS formulation was assessed. Promising results were observed as there was a significant increase ($p<0.05$) on drug intracellular/cell levels for the nanoPS system after 0.5 h. It was observed a RIF increment from 1.99 to 6.92 µg/mg (3.5-fold) for the drug control and the RIF-loaded nanoPS, respectively (**Fig. 4**). Afterwards, the RIF content was decreased being the drug intracellular/cell level of 2.86 µg/mg after 6 h, representing a 2-fold increment versus the RIF control

(**Fig. 4**). The drug accumulation on macrophage cytosol could enhance the conventional oral/parenteral anti-TB therapy, improving patient adherence and minimizing the development of *M. tuberculosis* resistance.

4. Conclusions

In this study, we developed a clinically relevant PEG-PCL-based nano-sized PS formulation loaded with RIF (up to 4.62 mg/mL). Our unique nanoPS dispersion showed an excellent colloidal stability in aqueous media and exhibited an enhanced drug accumulation in murine macrophages, representing a novel nanotechnological platform for its potential application in TB respirable therapy. It is worth stressing that TB pulmonary drug delivery has been in the spotlight as an alternative administration route over the last decade. In this context, we report for the first time a novel nano-sized PS-based formulation employing a first-line anti-TB drug for its use in TB field.

Future experiments will be focused on the drug-loaded nanoPS aerodynamic diameter as well as on *in vivo* studies, with the objective of investigating the possible involved uptake mechanism.

Acknowledgements

Authors thank the University of Buenos Aires (Grant UBACyT 20020130200038BA and UBACYT 20020130200005BA). Marcela A. Moretton, Lorena Gonzalez and Diego A. Chiappetta are staff-members of CONICET, Argentina. Ezequiel Bernabeu is supported by postdoctoral scholarship of CONICET, Argentina. Maximiliano Cagel is supported by a Ph.D. scholarship of CONICET, Argentina.

References

[1] http://www.who.int/mediacentre/factsheets/fs104/en/ (accessed September 2015).

[2] http://www.who.int/tb/strategy/en/ (accessed September 2015).

[3] G. Sotgiu, R. Centis, L. D'ambrosio, G. Battista Migliori, Cold Spring Harb. Perspect. Med. (2015), http://dx.doi.org/10.1101/cshperspect.a017822

[4] L.C. du Toit, V. Pillay, M.P. Danckwerts, Respir Res 7 (2006) 118.

[5] Treatment of tuberculosis guidelines, WHO Report, 4th ed., 2010. http://whqlibdoc.who.int/publications/2010/9789241547833_eng.pdf

[6] U.U. Shah, M. Roberts, M.O. Gul, C. Tuleu, M.W. Beresford, Int. J. Pharm. 416 (2011) 1.

[7] Global tuberculosis report, WHO Report, 2014. (http://apps.who.int/iris/bitstream/10665/137094/1/9789241564809_eng.pdf)

[8] F. Andrade, D. Rafael, M. Videira, D. Ferreira, A. Sosnik, B. Sarmento, Adv Drug Del 65 (2013) 1816.

[9] D-D. Pham, E. Fattal, N. Tsapis, Int. J. Pharm. 478 (2015) 517.

[10] J.S. Patton, C.S. Fishburn, J.G. Weers, Proc. Am. Thorac. Soc. 1 (2004) 338.

[11] O. Taratula, O.B. Garbuzenko, A.M. Chen, T. Minko, J Drug Targeting 19 (2011) 900.

[12] R. Savlaa, T. Minko, J Drug Targeting 21(2013) 925.

[13] M.A. Boks, W.W.J. Unger, S. Engels, M. Ambrosini, Y. van Kooyk, R. Luttge, Int. J. Pharm. 491 (2015) 375.

[14] W. Wang, R. Zhu, Q. Xie, A. Li, Y. Xiao, H. Liu, D. Cui, Y. Chen, S. Wang, Int J Nanomed 7 (2012) 3667.

[15] J.S. Lee, J. Feijen, J Control Release 161 (2012) 473.

[16] J. Liao, C. Wang, Y. Wang, F. Luo, Z. Qian, Curr Pharm Des 18 (2012) 3432.

[17] H-Y. Chang, Y-J. Sheng, H-K. Tsao, Soft Matter 10 (2014) 6373.

[18] M. Massignani, H. Lomas, G. Battaglia, Adv Polym Sci 229 (2010) 115.

[19] J-F. Le Meins, O. Sandre, S. Lecommandoux, Eur Phys J E Soft Matter 34 (2011) 14.

[20] S-P. Hsu, I-M. Chu, J-D. Yang, J Appl Polym Sci 125 (2012) 133.

[21] D.D. Lane, F.Y. Su, D.Y. Chiu, S. Srinivasan, J.T. Wilson, D.M. Ratner, P.S. Stayton, A.J. Convertine, Polym Chem 6 (2015) 1255.

[22] W-C. Huang, Y-C. Chen, Y-H. Hsu, W-Y. Hsieh, H-C. Chiu, Colloids Surf. B Biointerfaces 128 (2015) 67.

[23] X. Wen, Y. Wang, F. Zhang, X. Zhang, L. Lu, X. Shuai, J. Shen, Biomaterials 35 (2014) 4627.

[24] R. Nahire, M.K. Haldar, S. Paul, A.H. Ambre, V. Meghnani, B. Layek, K.S. Katti, K.N. Gange, J. Singh, K. Sarkar, S. Mallik, Biomaterials 35 (2014) 6482.

[25] Y. Yu, X. Jiang, S. Gong, L. Feng, Y. Zhong, Z. Pang, Nanoscale 6 (2014) 3250.

[26] I. P. Kaur, H. Singh, J Control Release 184 (2014) 36.

[27] M.A. Moretton, R.J. Glisoni, D.A. Chiappetta, A. Sosnik, Colloids Surf. B Biointerfaces 79 (2010) 467.

[28] E. Bernabeu, L. Gonzalez, M.J. Legaspi, M.A. Moretton, D.A. Chiappetta, J Nanosci Nanotechnol (2015) doi:10.1166/jnn.2015.10739.

[29] M.A. Moretton, D.A. Chiappetta, F. Andrade, J. das Neves, D. Ferreira, B. Sarmento, A. Sosnik, J Biomed Nanotechnol 9 (2013) 1076.

[30] Q. Liu, R-T. Li, H-Q. Qian, M. Yang, Z-S. Zhu, W. Wu, X-P. Qian, L-X. Yu, X-Q. Jiang, B-R. Liu, Int J Nanomed 7 (2012) 281.

[31] K. Letchford, H. Burt, Eur J Pharm Biopharm 65 (2007) 259.

[32] F. Ahmed, D.E. Discher, J Control Release 96 (2004) 37.

[33] S. Rameez, H. Alosta, A.F. Palmer, Bioconjugate Chem 19 (2008) 1025.

[34] L. Zhang, Y. He, G. Ma, C. Song, H. Sun, Nanomedicine 8 (2012) 925.

[35] K. Kita-Tokarczyk, J. Grumelard, T. Haefele, W. Meier, Polymer 46 (2005) 3540.

[36] C. Sanson, C. Schatz, J-F. Le Meins, A. Brûlet, A. Soum, S. Lecommandoux, Lagmuir 26 (2010) 2751.

[37] J.P. Jain, W.Y. Ayen, N. Kumar, Curr Pharm Des 17 (2011) 65.

[38] J.C-M. Lee, H. Bermudez, B.M. Discher, M.A. Sheehan, Y-Y. Won, F.S. Bates, D.E. Discher, Biotechnol Bioeng 73 (2001) 135.

[39] G. Battaglia, A.J. Ryan, Macromolecules 39 (2006) 798.

[40] L. Ma, A. Eisenberg, Lagmuir 25 (2009) 13730.

[41] G.D. Pangu, K.P. Davis, F.S. Bates, D.A. Hammer, Macromol Biosci 10 (2010) 546.

[42] M. Hoppentocht, P. Hagedoorn, H.W. Frijlink, A.H. de Boer, Eur J Pharm Biopharm 86 (2014) 23.

[43] M.C. Gohel, K.G. Sarvaiya, AAPS PharmSciTech 8 (2007) Article 68.

[44] M. González-Juarrero, M.P. O'Sullivan, Tuberculosis 91 (2011) 86.

[45] G.G. Gallo, P. Radaelli, En: K. Florey (Ed), "Analytical Profiles of Drug Subtances", vol. 5, Academic Press Inc., Florida, EEUU, 467 (1987).

[46] R. Sharma, D. Saxena, A. K. Dwivedi, A. Misra, Pharm Res 18 (2001) 1405.

[47] S.K. Katiyar, S. Bihari, S. Prakash, J Postgrad Med 54 (2008) 245.

[48] A. Ari, J.B. Fink, Expert Rev. Respir. Med. 7 (2013) 665.

[49] W.S. Cheow, M.L. Ling Ng, K. Kho, K. Hadinoto, Int J Pharm 404 (2011) 289.

[50] S.A. Meenach, K.W. Anderson, J.Z. Hilt, R.C. McGarry, H.M. Mansour, Eur J Pharm Sci 49 (2013) 699.

[51] L. Jia, D. Cui, J. Bignon, A. Di Cicco, J. Wdzieczak-Bakala, J. Liu, M-H. Li, Biomacromolecules 15 (2014) 2206.

[52] H.L. Jiang, M.L. Kang, J.S. Quan, S.G. Kang, T. Akaike, H.S. Yoo, c. S. Cho, Biomaterials 29 (2008) 1931.

[53] G. Battaglia, A.J. Ryan, J Am Chem Soc, 127 (2005) 8757.

[54] A. Verma, F. Stellacci, Small 6 (2010) 12.

[55] O. Onaca, R. Enea, D.W. Hughes, W. Meier, Macromol Biosci 9 (2009) 129.

[56] L.E. DesJardin, T.M. Kaufman, B. Potts, B. Kutzbach, H. Yi, L.S. Schlesinger, Microbiology 148 (2002) 3161.

[57] S. Prior, B. Gander, N. Blarer, H.P. Merkle, M.L. Subira, J.M. Irache, C. Gamazo, Eur J Pharm Sci 15 (2002) 197.

Table 1. PEG-PCL block copolymers synthesized by ROP and their PEG precursors.

Sample	CL/EO[a] Molar ratio	M_n[a] (KDa)	f_{PEG}[b] (%)	T_m[c] (°C)	ΔH_m[c] (J/g)
mPEG 5000	-	-	-	62	185.2
di-PCL(7200)[d]	0.56	12.2	40.9	58	103.3
di-PCL(12800)[d]	0.99	17.8	28.1	59	86.9
PEG(4000)	-	-	-	58	133.3
tri-PCL(4000)[e]	0.77	12.2	33.3	56	47.0
PEG(6000)	-	-	-	63	214.8
tri-PCL(6000)[e]	0.77	17.9	33.3	57	48.2
PEG(10000)	-	-	-	60	191.7
tri-PCL(10000)[e]	0.77	30.1	33.3	58	87.7

[a] Calculated by ^{1}HRMN.
[b] Hydrophilic block per total copolymer mass.
[c] Calculated by DSC.
[d] Di-block mPEG-PCL.
[e] Tri-block PCL-PEG-PCL.

Table 2. Size and size distribution (PDI) data of RIF-free nanoPS (1% w/v) obtained by phase inversion in absence and presence of sonication over 14 days (n=3±S.D.)

Sample	Time (h)	Sonication	D_h (nm) (±SD)				PDI (±SD)
			Peak 1[a]	*%*	*Peak 2*[b]	*%*	
di-PCL(7200)	0	-	66.3 (3.3)	100.0	-	-	0.186 (0.009)
		√	71.8 (3.1)	100.0	-	-	0.176 (0.008)
	3	-	74.5 (1.2)	100.0	-	-	0.185 (0.008)
		√	77.7 (3.6)	100.0	-	-	0.188 (0.013)
	7	-	76.9 (6.1)	100.0	-	-	0.211 (0.006)
		√	83.5 (5.8)	100.0	-	-	0.194 (0.011)
	14	-	82.2 (10.3)	100.0	-	-	0.280 (0.021)
		√	84.5 (1.9)	100.0	-	-	0.208 (0.002)
di-PCL(12800)	0	-	72.8 (3.0)	100.0	-	-	0.134 (0.011)
		√	81.3 (4.9)	100.0	-	-	0.147 (0.005)
	3	-	77.3 (1.8)	100.0	-	-	0.127 (0.008)
		√	85.9 (0.9)	100.0	-	-	0.127 (0.006)
	7	-	82.5 (1.5)	100.0	-	-	0.123 (0.016)
		√	93.1 (3.1)	100.0	-	-	0.135 (0.006)
	14	-	91.1 (5.2)	100.0	-	-	0.221 (0.004)
		√	100.5 (2.8)	100.0	-	-	0.155 (0.008)
tri-PCL(4000)	0	-	92.8 (6.5)	100.0	-	-	0.338 (0.003)
		√	67.3 (1.4)	51.6	275.2 (3.0)	48.4	0.414 (0.011)
	3	-	152.5 (19.4)	100.0	-	-	0.329 (0.043)
		√	159.8 (0.5)	100.0	-	-	0.407 (0.000)
	7	-	68.4 (5.6)	47.1	283.3(2.3)	52.9	0.627 (0.060)
		√	58.6 (7.5)	35.7	227.9 (27.6)	64.3	0.396 (0.001)
	14	-	>6µm	-	-	-	-
		√	>6µm	-	-	-	-
tri-PCL(6000)	0	-	75.6 (3.3)	100.0	-	-	0.250 (0.011)
		√	57.2 (1.5)	25.8	368.5(21.5)	74.2	0.513 (0.020)
	3	-	112.8 (10.6)	100.0	-	-	0.610 (0.024)
		√	118.4(12.0)	48.8	688.2(17.3)	51.2	0.643 (0.081)
	7	-	79.9 (10.0)	26.3	1839 (200.3)	73.7	1.000 (0.002)
		√	106.1 (10.4)	5.4	3062.0 (100.2)	94.6	0.507 (0.030)
	14	-	>6µm	-	-	-	-
		√	>6µm	-	-	-	-
tri-PCL(10000)	0	-	75.7 (0.5)	100.0	-	-	0.174 (0.009)
		√	73.0 (5.4)	32.3	373.0(18.3)	67.7	0.465 (0.006)
	3	-	82.1 (0.6)	100.0	-	-	0.178 (0.006)
		√	70.1 (3.1)	29.8	360.1 (4.5)	70.2	0.464 (0.007)
	7	-	82.3 (3.0)	100.0	-	-	0.191 (0.006)
		√	65.2 (2.8)	28.9	323.1 (10.1)	71.1	0.470 (0.004)
	14	-	89.8 (3.6)	100.0	-	-	0.206 (0.008)
		√	313.0 (35.0)	83.7	2192 (299.0)	16.3	0.428 (0.040)

PDI: polydispersity index
[a] *Peak 1* corresponds to the fraction of smaller size.
[b] *Peak 2* corresponds to the fraction of larger size.

Table 3. Size and size distribution (PDI) data of RIF-loaded nanoPS (1% w/v) over 14 days (n=3±S.D.)

Sample	Time (h)	D_h (nm) (±SD)		PDI (±SD)
		Peak	*%*	
di-PCL(7200)	0	76.0 (2.3)	100.0	0.138 (0.014)
	3	75.0 (2.3)	100.0	0.134 (0.019)
	7	73.3 (2.0)	100.0	0.126 (0.014)
	14	72.8 (2.3)	100.0	0.140 (0.008)
di-PCL(12800)	0	84.6 (3.3)	100.0	0.150 (0.003)
	3	83.7 (0.7)	100.0	0.110 (0.004)
	7	84.2 (0.6)	100.0	0.118 (0.037)
	14	97.8 (4.6)	100.0	0.174 (0.005)
tri-PCL(4000)	0	65.8 (3.7)	100.0	0.161 (0.016)
	3	67.7 (0.8)	100.0	0.191 (0.005)
	7	63.7 (2.0)	100.0	0.174 (0.006)
	14	66.1 (1.2)	100.0	0.205 (0.006)
tri-PCL(6000)	0	67.0 (1.2)	100.0	0.168 (0.004)
	3	65.7 (1.2)	100.0	0.159 (0.014)
	7	63.9 (0.6)	100.0	0.171 (0.002)
	14	102.2 (2.8)	100.0	0.181 (0.008)
tri-PCL(10000)	0	94.0 (2.4)	100.0	0.142 (0.013)
	3	91.4 (0.9)	100.0	0.131 (0.018)
	7	91.0 (2.4)	100.0	0.137 (0.006)
	14	97.5 (4.0)	100.0	0.157 (0.018)

PDI: polydispersity index

Table and Figure captions

Table 1. PEG-PCL block copolymers synthesized by ROP and their PEG precursors.

Table 2. Size and size distribution (PDI) data of RIF-free nanoPS (1% w/v) obtained by phase inversion in absence and presence of sonication over 14 days (n=3±S.D.)

Table 3. Size and size distribution (PDI) data of RIF-loaded nanoPS (1% w/v) over 14 days (n=3±S.D.)

Figure 1 Chemical structures of di-block (mPEG-PCL) and tri-block (PCL-PEG-PCL) derivatives.

Figure 2 TEM micrograph of RIF-loaded tri-PCL(4000) nanoPS 1% w/v in distilled water and negatively stained with phosphotungstic acid solution (1% w/v). Scale bar = 200 nm. Photo inset: magnification of nanoPS where arrows point out two different vesicle domains.

Figure 3 *In vitro* drug release profiles of RIF-loaded nanoPS dispersions (1% w/v) at 37°C over 6 h (n=3±S.D.)

Figure 4 Time-dependent intracellular/cell RIF levels in RAW 264.7 cell line for drug-loaded tri-PCL(4000) nanoPS in comparison with RIF aqueous solution. RIF amount was normalized by protein concentrations of the cell lysates. Results are expressed as mean±S.D. (n = 3).

★ The intracellular/cell RIF levels are significantly ($p<0.05$) higher for nanoPS versus the drug control.

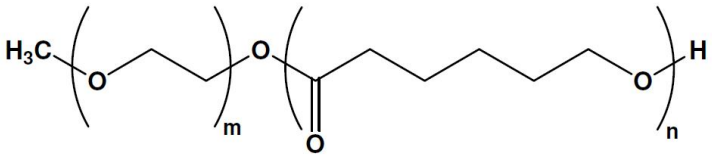

mPEG-PCL

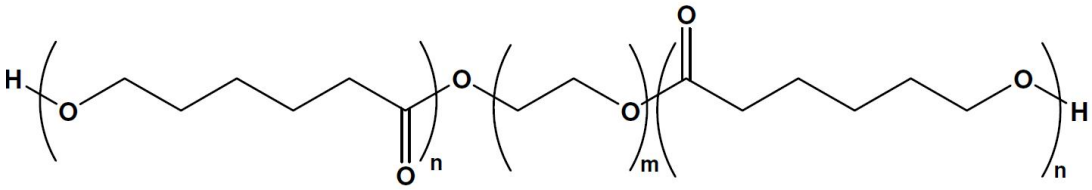

PCL-PEG-PCL